JOURNAL OF MATERIALS SCIENCE 27 (1992) 247–254

Preferred orientation of AlN plates prepared by chemical vapour deposition of $AlCl_3 + NH_3$ system

TAKASHI GOTO, JUN TSUNEYOSHI, KIYOSHI KAYA*, TOSHIO HIRAI
Institute for Materials Research, Tohoku University, 2-1-1 Katahira Sendai 980, Japan

Aluminium nitride (AlN) plates about 1 mm thick (maximum) were prepared by chemical vapour deposition (CVD) at the maximum deposition rate of 430 nm s^{-1} using $AlCl_3$, NH_3 and H_2 gases at deposition temperatures, T_{dep}, of 873–1473 K. The effects of deposition conditions on the preferred orientation, morphology and micro-structure were investigated. When T_{dep} was less than 1073 K, the resulting CVD AlN plates contained some impurity chlorine and the aluminium content exceed the nitrogen content. When T_{dep} exceeded 1173 K, no chlorine was detected, and the Al/N atomic ratio matched the stoichiometric value. The lattice parameters ($a = 0.311$ nm, $c = 0.4979$ nm) and density (3.26×10^3 kg m^{-3}) were in agreement with values reported previously. The crystal planes oriented parallel to the substrates changed from (1 1 $\bar{2}$ 0) to (1 0 $\bar{1}$ 0) to (0 0 0 1) with increasing total gas pressure (P_{tot}) and decreasing T_{dep}. This tendency is discussed thermodynamically and is explained by the change of supersaturation in the gas phase.

1. Introduction

Aluminium nitride (AlN) films are potentially useful for electrical and optical devices because of their high thermal conductivity [1], excellent piezoelectricity [2] and high acoustic velocity [3]. In particular, because the acoustic velocity of AlN along the *c*-axis is fastest, the *c*-axis of AlN films needs to be oriented parallel to substrates for application in surface acoustic wave (SAW) devices [3]. On the other hand, when the *c*-axis is oriented perpendicular to the substrates, the AlN films exhibit superior oxidation resistance [4]. Therefore, control of the preferred orientation is important in order to improve the properties of AlN films.

Several methods of preparing AlN films have been reported, including reactive sputtering [5], reactive molecular epitaxy [6] and chemical vapour deposition (CVD) [8–14]. However, CVD technique is known to be the most suitable in controlling the preferred orientation [7]. CVD AlN films have been prepared in the past by using $AlCl_3 + NH_3$ [8–11], $AlBr_3 + NH_3$ [12], $AlCl_3 \cdot xNH_3$ adduct compounds [13, 14] and $Al(CH_3)_3 + NH_3$ [15] as source materials. Among these, single-crystal CVD AlN films prepared on silicon single-crystal substrates, had epitaxial relationships of Si(1 1 1)//AlN(0 0 0 1), Si[2 2 0]//AlN[1 1 $\bar{2}$ 0] [8], while AlN films obtained on Al_2O_3 single crystal had Al_2O_3(0 0 0 1)//AlN(0 0 0 1), Al_2O_3[0 1 $\bar{1}$ 0]//AlN[$\bar{2}$ 1 1 0] [14] relationship. When polycrystalline CVD AlN films were prepared on graphite substrates, the resulting films showed the dominant orientation in (1 1 $\bar{2}$ 0) and (1 0 $\bar{1}$ 3) planes [10] and (0 0 0 1) planes [4, 11]. However, the effects of CVD conditions on the outcome of the preferred orientation have never been fully investigated.

In the present work the optimum CVD conditions for preparing high-purity and high-density AlN plates were explored, and the relationship between CVD conditions and preferred orientation of the resulting films was investigated. $AlCl_3$ was chosen as the aluminium source material because other aluminium source materials such as $AlBr_3$, $AlCl_3 \cdot xNH_3$ adducts and $Al(CH_3)_3$ easily decompose at less than 1000 K and thus the observation of the effects of CVD conditions over wide temperature ranges becomes impossible.

2. Experimental procedure

Fig. 1 shows a schematic diagram of the CVD apparatus. An inductively heated cold-wall-type CVD furnace was used. Hydrogen gas (99.99%), ammonia gas (99.5%) and anhydrous $AlCl_3$ powder (98%) were used as source materials. The $AlCl_3$ reservoir was maintained at 405 K and hydrogen gas carried the $AlCl_3$ vapour into the CVD furnace. The equilibrium $AlCl_3$ vapour pressure at 405 K was about 2.7 kPa. The $AlCl_3$ vapour and ammonia gas were separately introduced into the CVD furnace through a double tube nozzle in order to prevent the formation of $AlCl_3 \cdot xNH_3$ ($x = 1$–3) adducts compounds. These source gases were mixed about 15 mm above the substrate. Graphite discs (20 mm diameter × 2 mm thick) were used as substrates.

The deposition temperatures, T_{dep}, were measured using a PtRh6%–PtRh30% thermocouple. Table I summarizes the CVD conditions.

* *Present address*: Asahi Chemical Industry Co. Ltd, Kawasaki 210, Japan.

0022–2461/92 $03.00 + .12

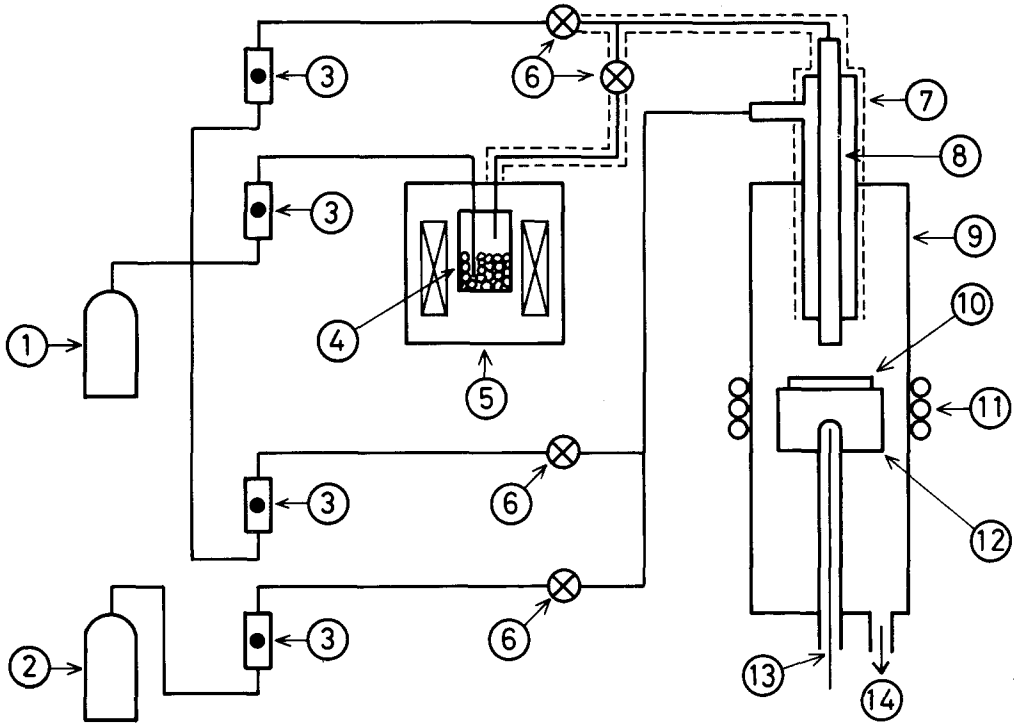

Figure 1 Schematic diagram of the CVD apparatus. 1, Hydrogen gas; 2, ammonia gas; 3, gas flow meter; 4, $AlCl_3$ reservoir; 5, constant-temperature bath; 6, valve; 7, ribbon heater; 8, quartz double-tube nozzle; 9, reaction chamber; 10, graphite substrate; 11, r.f. coil; 12, graphite susceptor; 13, thermocouple; 14, exhaust.

TABLE I Preparation conditions of CVD AlN

Deposition temperature, T_{dep}	873–1473 K
Total gas pressure, P_{tot}	0.4–101 kPa
Gas flow rates:	
H_2	1.7×10^{-5} m^3 s^{-1}
$AlCl_3$	5.5×10^{-9}–5.5×10^{-8} m^3 s^{-1}
NH_3	6.7×10^{-8}–6.7×10^{-7} m^3 s^{-1}
$NH_3/AlCl_3$	1.2, 6, 12
Deposition time	3.6–28.8 ks

The surface textures of deposits were observed by scanning electron microscopy. The preferred orientation and lattice parameters were evaluated by X-ray diffractometry (XRD, nickel-filtered CuK_α). The density was measured by the Archimedian method, with immersion in toluene. The aluminium and nitrogen contents were determined by chemical analyses. The chlorine impurity contents were determined by X-ray fluorescence analysis. The impurity content in AlN was determined from the relationship between the fluorescent intensity of chlorine and the chlorine content, using several mixtures of AlN and NaCl powders.

The supersaturation in the gas phase for the preparation of AlN by the CVD was calculated by the computer code SOLGASMIX-PV [16] using JANAF thermochemical data [17].

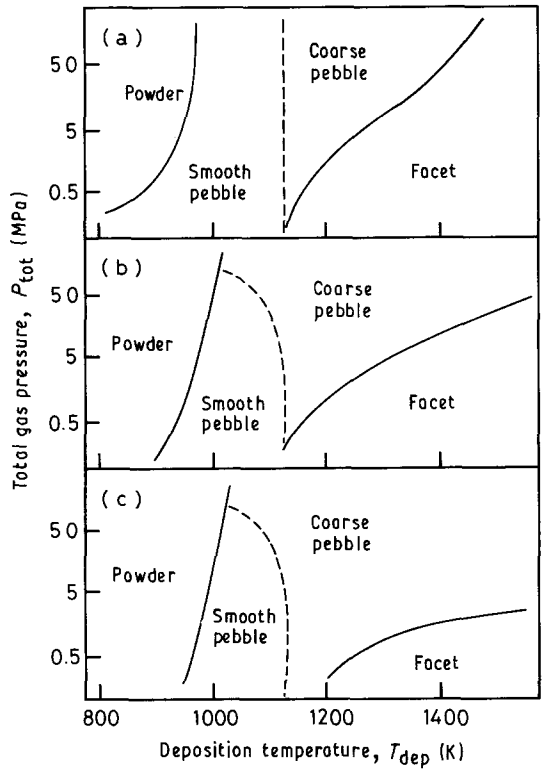

Figure 2 Typical surface textures of CVD AlN.
(a) "Powder", T_{dep} = 973 K, P_{tot} = 40 kPa, $NH_3/AlCl_3$ = 12.
(b) "Cone", T_{dep} = 1073 K, P_{tot} = 0.4 kPa, $NH_3/AlCl_3$ = 12.
(c) "Facet", T_{dep} = 1473 K, P_{tot} = 40 kPa, $NH_3/AlCl_3$ = 1.2.

3. Results and discussion

The surface textures of CVD AlN prepared in the present work were classified into three types: "powder", "pebble" and "facet". The "pebble" structure is further divided into "smooth pebble" and "coarse pebble" according to their surface. Typical surface textures observed by SEM are shown in Fig. 2. Fig. 3 summarizes the effects of CVD conditions on the morphology of CVD AlN. The "powder" region becomes smaller, and the "facet" region larger with

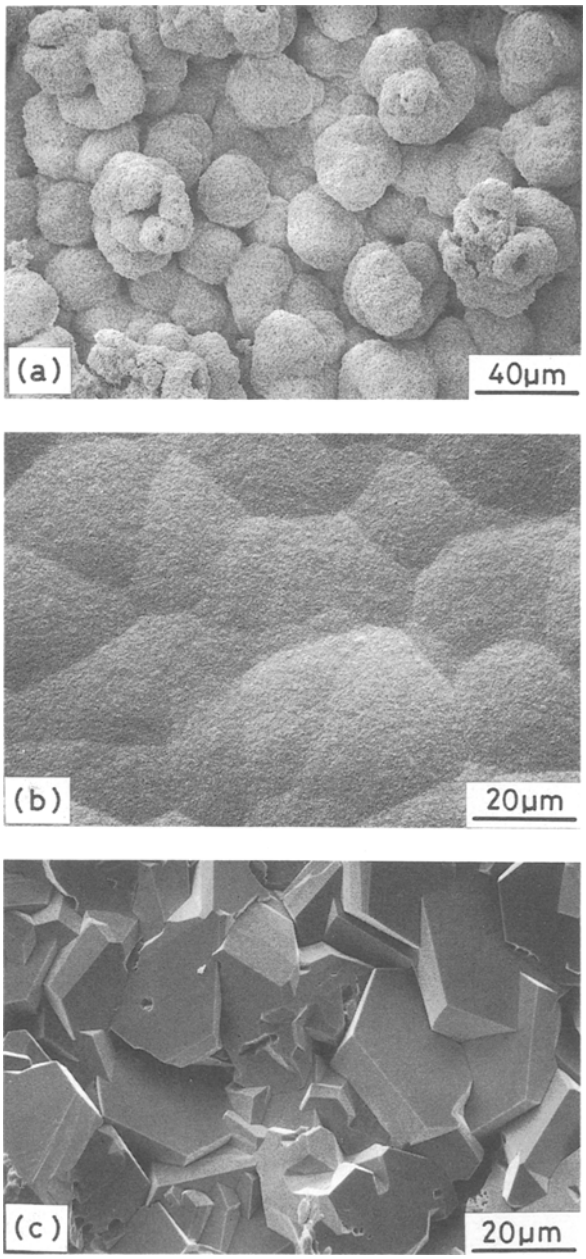

Figure 3 Effect of deposition temperature on surface textures at $NH_3/AlCl_3$ = (a) 1.2, (b) 6 and (c) 12.

decreasing $NH_3/AlCl_3$. For all cases examined, the boundaries between either "smooth pebble" and "coarse pebble" or "facet" were observed at about T_{dep} = 1123 K. The deposits having "smooth pebble" structure were transparent, while the "coarse pebble" and "facet" deposits were opaque and their colours changed from brown to grey with increasing $NH_3/AlCl_3$. Suzuki and Tanji [10] reported the effects of CVD conditions on the morphology of CVD AlN prepared from the $AlCl_3 + NH_3$ system. They showed that powders formed at P_{tot} = 133 Pa and T_{dep} = 873 K, changed from "dome cone" to "pyramid cone" to "plate column" to "coarse column" with increasing T_{dep} in the $NH_3/AlCl_3$ range of 1–4. This trend is nearly in agreement with the present results shown in Fig. 3.

It is known that the morphology of CVD materials varies with T_{dep} and supersaturation. At a given supersaturation the morphology varies from "powder" to "fine-grained polycrystalline" to "coarse-grained polycrystalline" to "dendritic polycrystalline" to "single crystalline" with increasing T_{dep} [7]. The morphological change shown in Fig. 4, as well as that of Suzuki and Tanji [10], can be understood by the tendency mentioned above.

Fig. 4 shows the effect of T_{dep} on the chlorine impurity content. The impurity chlorine was only observed for the sample prepared at T_{dep} < 1073 K. The chlorine contents clearly increase with decreasing T_{dep} and $NH_3/AlCl_3$. The impurity chlorine was not detected for the samples prepared above T_{dep} = 1173 K by the X-ray fluorescence analysis. The chlorine counts observed were as small as the instrument noise level. The same trend was also observed with the change of $NH_3/AlCl_3$ ratio in the range 6–12.

Fig. 5 shows the effect of T_{dep} on the contents of aluminium and nitrogen. The stoichiometric levels of aluminium (65.8 wt %) and nitrogen (34.2 wt %) are indicated in Fig. 5 by arrows. The aluminium contents were almost constant throughout the temperature examined and agreed well with the stoichiometric composition. The nitrogen contents slightly decreased with decreasing T_{dep} below T_{dep} = 1073 K; however, above T_{dep} = 1173 K the nitrogen contents were

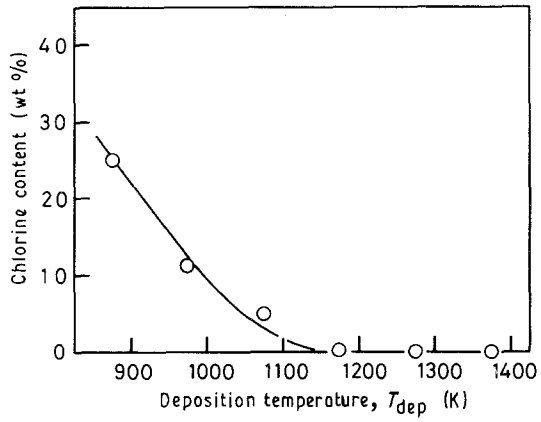

Figure 4 Effect of deposition temperature on impurity chlorine content at P_{tot} = 4 kPa and $NH_3/AlCl_3$ = 1.2.

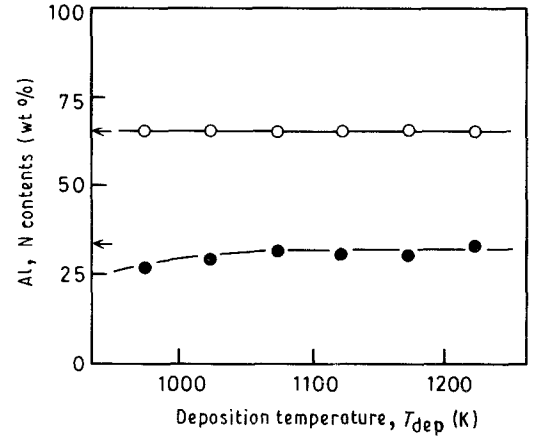

Figure 5 Effect of deposition temperature on the composition of (○) aluminium and (●) nitrogen at P_{tot} = 4 kPa, $NH_3/AlCl_3$ = 1.2. The arrows indicate the stoichiometric composition.

stoichiometric and independent of T_{dep}. These results suggest a possibility that the impurity chlorine atoms substitutionally replace the lattice sites on nitrogen. The CVD AlN plates prepared at $T_{dep} > 1173$ K had a stoichiometric composition independent of $NH_3/AlCl_3$ and P_{tot}.

No known reports on the impurity chlorine analysis for CVD AlN are available; however, Pauleau *et al.* [12] examined impurity bromine using the Rutherford back-scattering (RBS) method for the CVD AlN films prepared from the $AlBr_3 + NH_3$ system. According to Pauleau *et al.* [12], the bromine content in the deposits prepared at $T_{dep} = 723$ K was about 5×10^{16} atoms cm^{-2} and decreased with increasing T_{dep}. No bromine atoms were detected in deposits prepared above $T_{dep} = 923$ K. This trend is in agreement with the present results.

In the past, the density and lattice parameters of CVD AlN have not been reported. Fig. 6 shows the effect of T_{dep} on the density. A theoretical density (3.26×10^3 kg m^{-3} [18]) is indicated by an arrow and denoted TD in Fig. 6. The density as well as the composition of the CVD AlN plates prepared above $T_{dep} = 1173$ K are in good agreement with the theoretical values. However, when T_{dep} was less than 1073 K the density decreased to about 90% theoretical. The density of CVD AlN plates was independent of P_{tot} and $NH_3/AlCl_3$ in the range examined in this study.

Fig. 7 shows the effect of T_{dep} on lattice parameter. The arrows in Fig. 7 show the values of JCPDS cards ($a = 0.3111$ nm, $c = 0.4979$ nm [19]). The a and c values of CVD AlN plates prepared above $T_{dep} = 1173$ K are in good agreement with the literature values independent of P_{tot} and $NH_3/AlCl_3$; however, those values below $T_{dep} = 1073$ K showed much larger density than those reported in the literature.

There have been no reports on the bonding state of impurity chlorine, but the impurity bromine is known to combine with aluminium atoms. As was mentioned earlier, the impurity chlorine must combine with aluminium atoms by substituting nitrogen atoms. This substitution of chlorine atoms for nitrogen atoms might be the reason for the trend of increasing lattice parameters with decreasing T_{dep}.

Fig. 8 shows the effect of T_{dep} on the deposition rate constants. Because the growth rates in thickness of CVD AlN plates were constant during the deposition periods, the deposition rate constant was determined by the weight increase per unit time and unit substrate area. At $T_{dep} < 1073$ K, the deposition rate constants increased linearly with increasing T_{dep}, and the

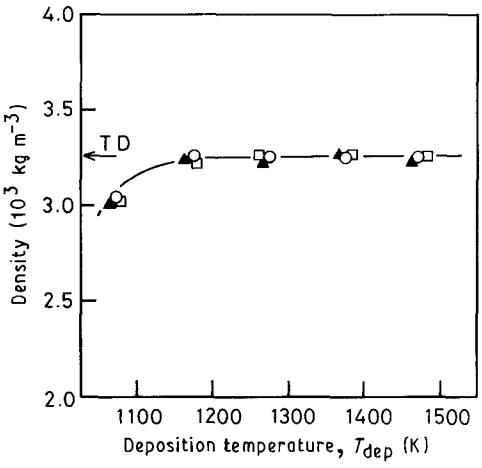

Figure 6 Effect of deposition temperature on density at $P_{tot} = 4$ kPa. TD = theoretical density. $NH_3/AlCl_3$: (○) 1.2, (▲) 6, (□) 12.

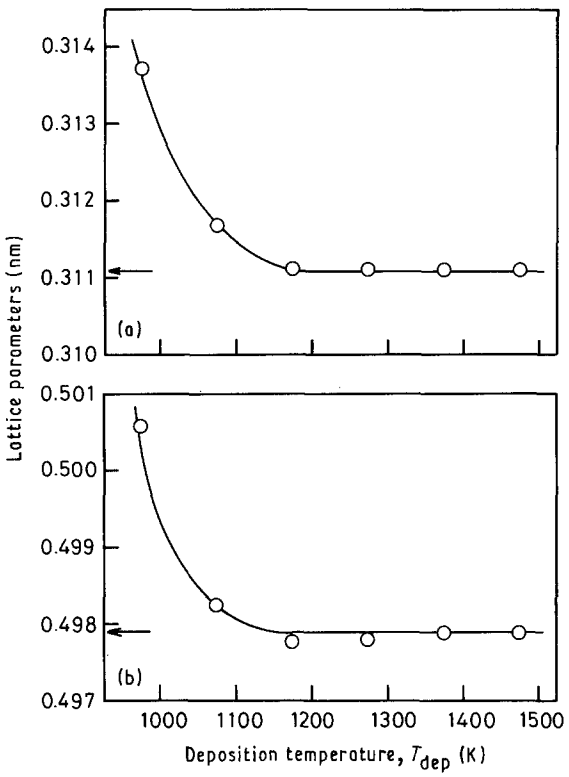

Figure 7 Effect of deposition temperature on lattice parameters (a) a, (b) c, at $P_{tot} = 4$ kPa, $NH_3/AlCl_3 = 1.2$. The arrow indicates a literature value [19].

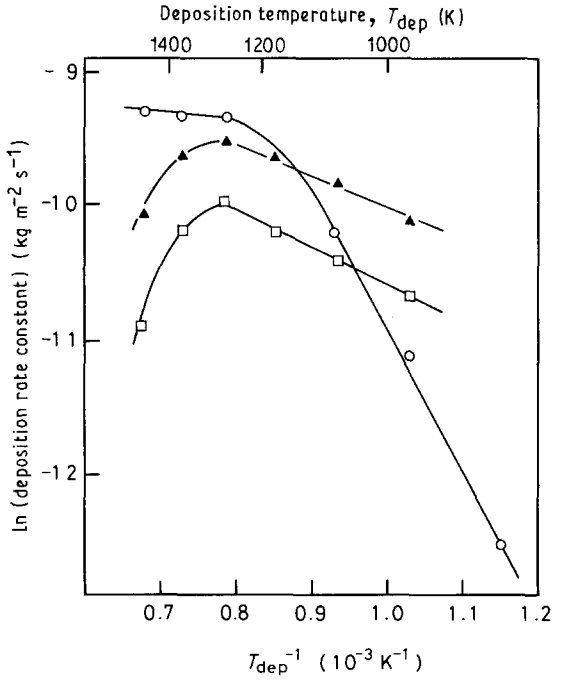

Figure 8 Effect of deposition temperature on deposition rate constant at $NH_3/AlCl_3 = 1.2$. P_{tot}: (○) 4 kPa, (▲) 40 kPa, (□) 101 kPa.

TABLE II Preparation conditions and maximum growth rates of CVD AlN films

Source gases	Deposition temperature (K)	Total gas pressure (kPa)	Maximum growth rate ($nm\,s^{-1}$)	Reference
$AlCl_3 + NH_3$	1173–1623	2	43	[8]
$AlCl_3 + NH_3$	973–1573	101	210	[9]
$AlCl_3 + NH_3$	873–1773	0.03–6.7	3600	[10]
$AlCl_3 + NH_3$	1003–1059	101	130	[11]
$AlCl_3 + NH_3$	1073–1473	101	3.4	[12]
$AlCl_3 + NH_3$	973–1673	0.7–1.3	910	[13]
$AlBr_3 + NH_3$	773–1173	101	8.6	[14]
$AlCl_3 + NH_3$	873–1173	0.4–101	430	Present work

calculated activation energy was $88\,kJ\,mol^{-1}$ at $P_{tot} = 0.4$ kPa; and $23\,kJ\,mol^{-1}$ at $P_{tot} = 40$ and 101 kPa. It is well known in the CVD process that when the activation energy is more than about $80\,kJ\,mol^{-1}$, the rate-controlling step is a chemical reaction, whereas when the energy is less than about $40\,kJ\,mol^{-1}$, some diffusion process in the gas phase is the rate-controlling step. The activation energy values of 88 and $23\,kJ\,mol^{-1}$ obtained in the present work may correspond well with the activation energies of a chemical reaction and diffusion process, respectively, but the details of the deposition mechanism remain uncertain. At a temperature above $T_{dep} = 1273$ K, the deposition rate constants were nearly constant at $P_{tot} = 4$ kPa, however, at $P_{tot} = 40$ and 101 kPa, they decreased with increasing T_{dep} as shown in Fig. 8. This phenomenon can be explained by the decrease in the deposition rate by formation of powder due to homogeneous nucleation in the gas phase at higher T_{dep} and P_{tot}. The T_{dep} where the maximum deposition rate constants occur decreased with increasing $NH_3/AlCl_3$. The maximum growth rate obtained in the present work was about $430\,nm\,s^{-1}$ ($120\,\mu m\,h^{-1}$) at $T_{dep} = 1473$ K, $P_{tot} = 4$ kPa and $NH_3/AlCl_3 = 1.2$, and under these conditions CVD AlN plates 1 mm thick were obtained. Past reports on deposition rates and preparation conditions for CVD AlN films are summarized in Table II. The maximum growth rate obtained in the present work was well below the value of $3600\,nm\,s^{-1}$ reported by Suzuki and Tanji [10], but was of the same order as those of other reports. Many parameters such as geometric configurations of the CVD apparatus, gas flow patterns around the substrates, mass flow rates of source gases, etc., might affect the difference between these growth rates.

Fig. 9 shows the relationship between CVD conditions and preferred orientation of the CVD AlN plates obtained in the present work. Suzuki and Tanji [10] reported that under any CVD conditions the dominant orientations were $(1\,1\,\bar{2}\,0)$ and $(1\,0\,\bar{1}\,3)$ planes parallel to the substrates. Itoh *et al.* [4] and Komiyama and Osawa [11] reported that the $(0\,0\,0\,1)$ oriented plane was the dominant orientation. However, the detailed relationships between CVD conditions and preferred orientation remains unexplained. In the present work, the $(0\,0\,0\,1)$ orientation was dominant at higher P_{tot} and changed to the $(1\,0\,\bar{1}\,1)$ orientation with decreasing P_{tot}. The $(1\,1\,\bar{2}\,0)$ orientation was dominant at higher T_{dep} and lower P_{tot}. This behaviour was observed to be almost independent of $NH_3/AlCl_3$.

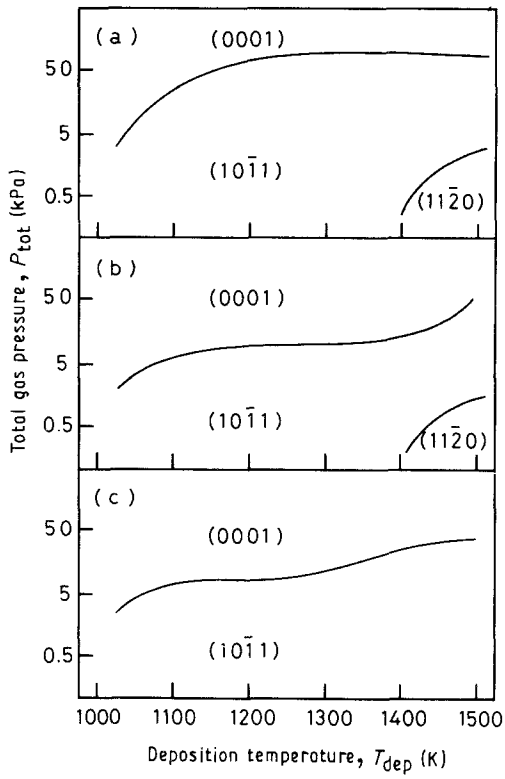

Figure 9 Relationship between CVD conditions and preferred orientation of CVD AlN plates at $NH_3/AlCl_3$ = (a) 1.2, (b) 6 and (c) 12.

Fig. 10 shows XRD patterns and Fig. 11 shows surface scanning electron micrographs of CVD AlN plates having the $(0\,0\,0\,1)$, $(1\,0\,\bar{1}\,1)$ and $(1\,1\,\bar{2}\,0)$ orientations. Many hexagonal facets which are characteristic of *c*-planes of hexagonal crystals were observed in the $(0\,0\,0\,1)$ oriented deposits. The morphology of the $(1\,0\,\bar{1}\,1)$ and $(1\,1\,\bar{2}\,0)$ oriented deposits is represented by the edges and/or ridges of the hexagons.

The preferred orientation in crystal growth from the vapour phase is widely known, and Bauer [21] and Evans and Wilman [22] presented some theoretical models for the preferred orientation of sputtered films. Mashita [23] reviewed their work, and the preferred orientation of many sputtered films has been explained. However, the preferred orientation for CVD

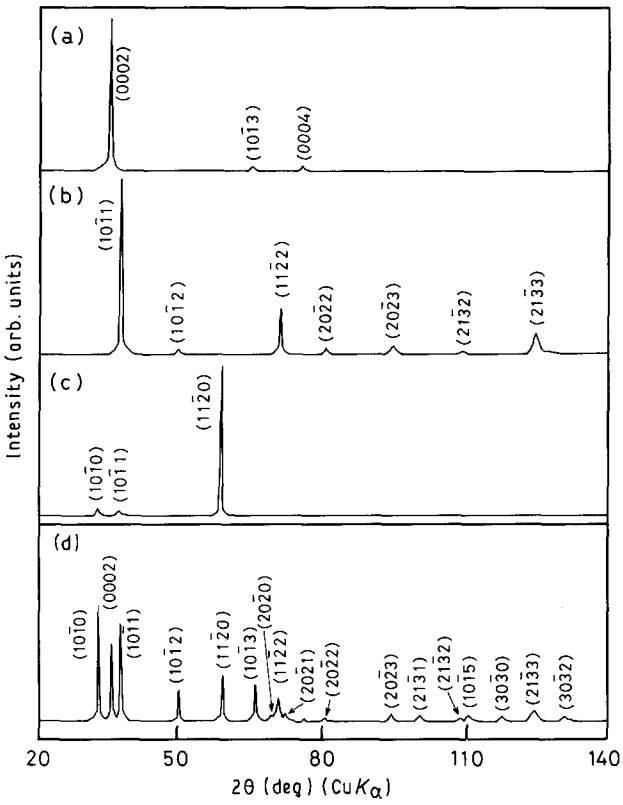

Figure 10 X-ray diffraction patterns of CVD AlN plates.
(a) (0 0 0 1) orientation, T_{dep} = 1273 K, P_{tot} = 101 kPa, $NH_3/AlCl_3$ = 6.
(b) (1 0 $\bar{1}$ 1) orientation, T_{dep} = 1373 K, P_{tot} = 0.4 kPa, $NH_3/AlCl_3$ = 1.2.
(c) (1 1 $\bar{2}$ 0) orientation, T_{dep} = 1473 K, P_{tot} = 0.4 kPa, $NH_3/AlCl_3$ = 1.2.
(d) AlN powder.

films is still not understood. The preferred orientation of CVD materials may be explained using the two-dimensional nuclei theory presented by Pangarov [24]. According to this model, the oriented planes are those where the nucleation energy to form a two-dimensional nucleus, W_{hkl}, is minimum. The W_{hkl} is defined by

$$W_{hkl} = \frac{B_{hkl}}{(1/mN)(\mu - \mu_0) - A_{hkl}} \quad (1)$$

where (hkl) are the Miller indices of the crystalline plane, μ is the chemical potential of the vapour phase, which is in equilibrium with the two-dimensional nucleus, μ_0 is the chemical potential of the vapour phase which is in equilibrium with the three-dimensional nucleus, m is the number of atoms in gas molecules, N is Avogadro's number, and A_{hkl} and B_{hkl} are both constants which vary depending on bonding strength between atoms in the crystal lattice. The W_{hkl}, which corresponds to the preferred orientation, varies with the supersaturation of the gas phase. Pangarov [25] calculated the relationships between W_{hkl} and supersaturation in many crystal lattice systems. According to the relationship for the hexagonal system given by Pangarov [25], the (0 0 0 1) orientation would be dominant at lower supersaturation and the preferred orientation would change from (0 0 0 1) to (1 0 $\bar{1}$ 1) to (1 1 $\bar{2}$ 0) with increasing supersaturation. Fig. 12 shows the effect of P_{tot} on the supersaturations of aluminium

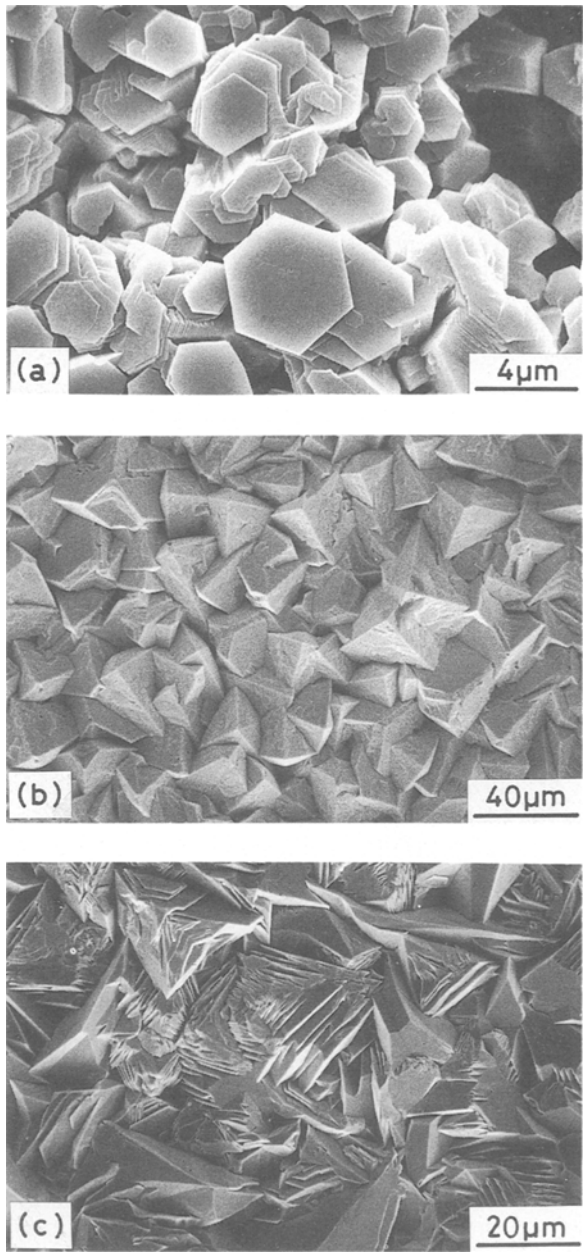

Figure 11 Surface textures of preferably oriented CVD AlN plates.
(a) (0 0 0 1) orientation, T_{dep} = 1273 K, P_{tot} = 101 kPa, $NH_3/AlCl_3$ = 6.
(b) (1 0 $\bar{1}$ 1) orientation, T_{dep} = 1373 K, P_{tot} = 4 kPa, $NH_3/AlCl_3$ = 1.2.
(c) (1 1 $\bar{2}$ 0) orientation, T_{dep} = 1473 K, P_{tot} = 0.4 kPa, $NH_3/AlCl_3$ = 12.

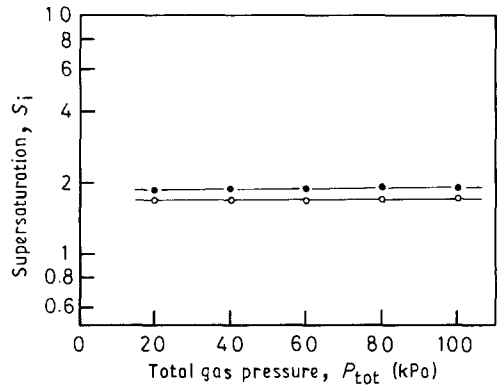

Figure 12 Effect of total gas pressure on supersaturations of (●) aluminium and (○) nitrogen species in the gas phase at T_{dep} = 1473 K and $NH_3/AlCl_3$ = 1.2.

and nitrogen at $T_{dep} = 1473$ K and $NH_3/AlCl_3 = 1.2$. The supersaturation, S_i, is defined as [26]

$$S_i = \frac{nP^{in}(i)}{\sum_j n_j P_j^{eq}(i)} \quad (2)$$

where S_i is the supersaturation of the ith atom, $P^{in}(i)$ is the partial pressure of source gas containing the ith atom, $P^{eq}(i)$ is the equilibrium partial pressure of gas species containing the ith atom, and j is the equilibrium gas species such as AlCl, $AlCl_3$, NH_2, NH_3, etc. n and n_j are the stoichiometric number of gases containing i atoms in input gases and in equilibrium phase, respectively. The supersaturations of both aluminium and nitrogen are almost independent of P_{tot} in the thermodynamic calculations. The same results were obtained for all other CVD conditions. However, collisions of molecules in the gas phase will increase with increasing P_{tot}, and these collisions accelerate the formation of by-products of NH_4Cl and $AlCl_3 \cdot xNH_3$ adducts shown in Equations 4a and b. Indeed the formation of a white powder was confirmed in the present experiments in the lower temperature region excluding the substrates.

$$AlCl_3 + NH_3 \rightarrow AlN + 3HCl \quad (3)$$

$$AlCl_3 + xNH_3 + 1/2\,H_2 \rightarrow NH_4Cl + AlCl_{3-x} \quad (4a)$$

$$AlCl_3 + xNH_3 \rightarrow AlCl_3 \cdot xNH_3 \quad (4b)$$

As shown in Fig. 8, the deposition rate constants decreased with increasing P_{tot} at temperatures below $T_{dep} = 1273$ K. As stated earlier, this decrease in rate constant must be due to the powder formation in the gas phase, and it is conceivable that this powder formation can significantly decrease the supersaturation in the gas phase. In preparing CVD Al_2O_3 films, Park *et al.* [27] reported similar results on the effect of P_{tot} on the supersaturation. They found that the supersaturation remained unchanged with the change in P_{tot}, as found in the present work. They speculated that the powder formation can cause changes in preferred orientation by decreasing the supersaturation. In the present work the preferred orientation changed from (1 1 $\bar{2}$ 0) to (1 0 $\bar{1}$ 1) to (0 0 0 1) with increasing P_{tot}. This result may be explained by the decrease in supersaturation in the gas phase. It has been reported that the characteristics of the preferred orientation of CVD TiC plates [26] and CVD TiB_2 [28] may be explained by the change in supersaturation in the gas phase.

The thermal conductivity of the CVD AlN plate obtained in the present work was 198 $W K^{-1} m^{-1}$ when the preferred orientation was (1 0 $\bar{1}$ 1). The measurement of the thermal conductivity for samples having other orientations was unsuccessful because the samples were too thin. The value of 198 $W K^{-1} m^{-1}$ was smaller than the theoretical value (320 $W K^{-1} m^{-1}$ [1]) as well as the value of single-crystalline AlN (250 $W K^{-1} m^{-1}$ [29]). These differences may have resulted from grain-boundary scattering. The present values are larger than the values of CVD AlN film (100–170 $W K^{-1} m^{-1}$) obtained by Hayashi *et al.* [30]. They reported that the lattice defects and/or impurity oxygen might have decreased the thermal conductivity of their CVD AlN films.

4. Conclusions

AlN plates were prepared by CVD using $AlCl_3 + NH_3 + H_2$ as source gases. The following results were obtained.

1. The surface textures of CVD AlN plates varied from "powder" to "smooth pebble" to "coarse pebble" to "facet" with increasing T_{dep} and decreasing P_{tot}.
2. Impurity chlorine was not detected and the compositions of aluminium and nitrogen were stoichiometric in CVD AlN plates prepared at temperatures above $T_{dep} = 1173$ K. Impurity chlorine was observed in the CVD AlN plates prepared below $T_{dep} = 1073$ K. Chlorine contents increased from 5 to 25 wt % with decreasing T_{dep}.
3. The lattice parameters of CVD AlN plates prepared above $T_{dep} = 1173$ K were $a = 0.311$ nm, $c = 0.4979$ nm, and their density was 3.26×10^3 kg m^{-3}. These were in agreement with past literature values. The lattice parameters of CVD AlN plates prepared at below $T_{dep} = 1073$ K were larger and their densities were smaller than literature values. This phenomenon suggests that chlorine atoms combine with aluminium atoms by substituting nitrogen sites.
4. The maximum growth rate was 430 nm s^{-1} at $T_{dep} = 1473$ K, $P_{tot} = 4$ kPa and $NH_3/AlCl_3 = 1.2$. Chlorine-free 1 mm thick CVD AlN plates were obtained.
5. The c-plane ((0 0 0 1)plane) of CVD AlN plates was oriented parallel to the substrates at $P_{tot} > 5$ kPa, independent of T_{dep}, and was oriented perpendicular to the substrates at about $T_{dep} = 1473$ K and $P_{tot} = 0.4$ kPa. The preferred orientation of CVD AlN plates varied depending on the CVD conditions. The preferred orientation of the CVD AlN plates changed from (1 1 $\bar{2}$ 0) to (1 0 $\bar{1}$ 1) to (0 0 0 1) with increasing P_{tot} and decreasing T_{dep}. This tendency was explained by the change of supersaturations of aluminium and nitrogen species in the gas phase.
6. The thermal conductivity of CVD AlN plates having (1 0 $\bar{1}$ 1) orientation was 198 $W K^{-1} m^{-1}$ at room temperature.

Acknowledgements

The authors thank M. Kishi, Seiko Electric Co. Ltd, for chlorine analysis. This research was supported in part by the Grant-in-Aid for Scientific Research from the Ministry of Education, Science and Culture, under Contract nos. 63 850 149 and 63 750 730.

References

1. G. A. SLACK, *J. Phys. Chem. Solids* **34** (1973) 321.
2. T. M. REEDER and D. K. WINSLOW, *IEEE Trans.* **MTT-17** (1967) 927.
3. E. STERN, *ibid.* **MTT-17** (1967) 927.
4. H. ITOH, M. KATO and K. SUGIYAMA, *Yogyo-Kyokai-Shi* **94** (1986) 145.

5. A. J. SHUSKUS, T. M. REEDER and E. L. PARADIS, *Appl. Phys. Lett.* **24** (1974) 155.
6. S. YOSHIDA, S. MISAWA, Y. FUJII, S. TAKEDA, H. HAYAKAWA, S. GONDA and A. ITOH, *J. Vac. Sci. Technol.* **16** (1979) 990.
7. W. A. BRYANT, *J. Mater. Sci.* **12** (1977) 1285.
8. A. J. NOREIKA and D. W. ING, *J. Appl. Phys.* **39** (1968) 5578.
9. J. BAUER, L. BISTE and D. BOLTZE, *Phys. Status Solidi (a)* **39** (1977) 173.
10. M. SUZUKI and H. TANJI, in "Proceedings of the 10th International Conference on Chemical Vapour Deposition", edited by G. Cullen (Electrochemical Society, Pennington, PA, 1987) p. 1089.
11. H. KOMIYAMA and O. OSAWA, *Jpn. J. Appl. Phys.* **24** (1985) L795.
12. Y. PAULEAU, A. BOUTEVILLE, J. J. HANTZPERQUE and J. C. REMY, *J. Electrochem. Soc.* **127** (1980) 1532.
13. T. L. CHU and R. W. KELM Jr, *ibid.* **122** (1975) 995.
14. D. W. LEWIS, *ibid.* **117** (1970) 798.
15. M. MORITA, N. UESUGI, S. ISOGAI, K. TSUBOUCHI and N. MIKOSHIBA, *Jpn. J. Appl. Phys.* **20** (1981) 17.
16. T. M. BESMANN, Oak Ridge National Laboratory report ORNL/TM-5775.
17. D. R. STULL and H. PROPHET (eds), "JANAF Thermochemical Tables", 2nd Edn, no. NSRDS-NMS-37 (US Government Printing Office, Washington DC, 1971).
18. K. M. TAYLOR and C. LENIE, *J. Electrochem. Soc.* **107** (1960) 308.
19. X-ray Powder Diffraction Files, JCPDS, (Swarthmore, USA, 1975) Card No. 25–1133.
20. L. M. IVANOVA and A. A. PLETYUSHKIN, *Izvest. Akademii Nauk SSSR, Neorg. Mater.* **3** (1967) 1817.
21. E. BAUER, in "Single Crystal Films", edited by H. Francombe and H. Sato (Pergamon Press, New York, 1964) p. 43.
22. D. M. EVANS and H. WILMAN, *Acta Crystallogr.* **5** (1952) 731.
23. M. MASHITA, *Surf. Sci.* **2** (1981) 46.
24. N. A. PANGAROV, *Electrochem. Acta* **7** (1962) 139.
25. *Idem, ibid.* **9** (1964) 721.
26. D. G. KIM, J. S. YOO and J. S. CHUN, *J. Vac. Sci. Technol.* **A4** (1986) 219.
27. C. S. PARK, J. G. KIM and J. S. CHUN, *J. Electrochem. Soc.* **130** (1983) 1607.
28. M. MUKAIDA, T. GOTO and T. HIRAI, *J. Mater. Sci.*, **25** (1990) 1069.
29. G. A. SLACK and T. F. McNELLEY, *J. Crystal Growth* **42** (1977) 560.
30. K. HAYASHI, T. OHASHI and T. HIRAO, "Abstracts 26th Symposium on Basic Science of Ceramics", Nagoya, 20–23 January 1988 (The Ceramic Society of Japan, 1988) p. 106.

Received 3 September 1990
and accepted 28 February 1991